Reaction Mechanisms

International Edition: DOI: 10.1002/anie.201410974
German Edition: DOI: 10.1002/ange.201410974

Ketene as a Reaction Intermediate in the Carbonylation of Dimethyl Ether to Methyl Acetate over Mordenite**

Dominik B. Rasmussen, Jakob M. Christensen, Burcin Temel, Felix Studt, Poul Georg Moses, Jan Rossmeisl, Anders Riisager, and Anker D. Jensen**

In memory of Haldor F. A. Topsøe

Abstract: *Unprecedented insight into the carbonylation of dimethyl ether over Mordenite is provided through the identification of ketene (CH_2CO) as a reaction intermediate. The formation of ketene is predicted by detailed DFT calculations and verified experimentally by the observation of doubly deuterated acetic acid (CH_2DCOOD), when D_2O is introduced in the feed during the carbonylation reaction.*

A number of acidic zeolites are selective catalysts for dimethyl ether (DME) carbonylation, and Mordenite has the highest activity.[1] However, the zeolite catalysts suffer from rapid deactivation because of a build-up of coke and larger carbonaceous species within the zeolite pores.[1c,2] The framework of Mordenite contains two types of cavities: eight-membered ring (8-MR) side pockets and 12-MR main channels. It has been reported that methyl acetate (MA) synthesis takes place within the 8-MR,[3] whereas the 12-MR has been suggested to be responsible for the coke formation which leads to catalyst deactivation.[2a,d] During the initial phase of DME carbonylation, DME reacts with the Brønsted sites, thus forming methyl groups and water [Eqs. (1) and (2)]:

$$CH_3OCH_3 + [SiO(H)Al] \rightleftharpoons [SiO(CH_3)Al] + CH_3OH \quad (1)$$

$$CH_3OH + [SiO(H)Al] \rightleftharpoons [SiO(CH_3)Al] + H_2O \quad (2)$$

These reactions, in which the Brønsted acid sites are methylated, give rise to an induction period. The steady-state phase involves the reaction of CO with the methyl groups, thus forming acetyl species, which in turn react with DME to produce MA and regenerate the methyl groups [Eqs. (3) and (4)]:

$$CO + [SiO(CH_3)Al] \rightarrow [SiO(COCH_3)Al] \quad (3)$$

$$CH_3OCH_3 + [SiO(COCH_3)Al] \rightarrow [SiO(CH_3)Al] + CH_3COOCH_3 \quad (4)$$

Experimental studies showed that formation of the acetyl species is the rate-limiting reaction step, and that the subsequent reaction between DME and acetyl is comparatively fast.[1a,b] Herein, we present unprecedented insights into the formation of acetyl over Mordenite in the steady-state phase, including the DFT energies and energy barriers for all reaction steps, and present experimental verification of the theoretical model by showing that ketene is a reaction intermediate as predicted by the DFT calculations.

We employ the BEEF-vdW functional,[4] which has been shown to quantitatively describe van der Waals interactions of molecules within zeolite pores,[5] as well as reaction kinetics.[6] Formation of the acetyl group was investigated for the 12-MR and 8-MR at the T1-O4 and T3-O3 sites, respectively (see Figure S1 in the Supporting Information, SI).[7] These sites are the preferred adsorption sites for methyl groups, as shown in Table S1 in the SI. The T3-O8 site in the 8-MR was found to be the most favorable adsorption site of methyl groups in previous DFT studies employing cluster models,[8] and for comparison we also investigated the formation of acetyl at this site (see Figures S2 and S3).

The reaction path for formation of acetyl, determined by DFT calculations, begins by the reaction of CO with a surface methyl group which yields an acetyl carbocation [Eq. (5)]:

$$CO + [SiO(CH_3)Al] \rightarrow CH_3CO^+\text{-}[SiOAl]^- \quad (5)$$

Figure 1 shows that the energy barrier for this step is 6 kJ mol^{-1} lower at T3-O3 (8-MR) than at T1-O4 (12-MR),

[*] D. B. Rasmussen, Prof. J. M. Christensen, Prof. A. D. Jensen
Department of Chemical and Biochemical Engineering
Technical University of Denmark
Building 229, 2800 Kgs. Lyngby (Denmark)
E-mail: jmc@kt.dtu.dk
aj@kt.dtu.dk
Dr. B. Temel, Dr. P. G. Moses
Haldor Topsøe Research Laboratories
Nymøllevej 55, 2800 Kgs. Lyngby (Denmark)
Dr. F. Studt
SUNCAT Center for Interface Science and Catalysis
SLAC National Accelerator Laboratory
2575 Sand Hill Road, Menlo Park, CA 94025 (USA)
Prof. J. Rossmeisl
Department of Physics, Technical University of Denmark
Building 307, 2800 Kgs. Lyngby (Denmark)
Prof. A. Riisager
Center for Catalysis and Sustainable Chemistry
Department of Chemistry, Technical University of Denmark
Building 207, 2800 Kgs. Lyngby (Denmark)

[**] This work was financed by the Technical University of Denmark and the Catalysis for Sustainable Energy Initiative (CASE) funded by the Danish Ministry of Science, Technology and Innovation.

Supporting information for this article is available on the WWW under http://dx.doi.org/10.1002/anie.201410974.

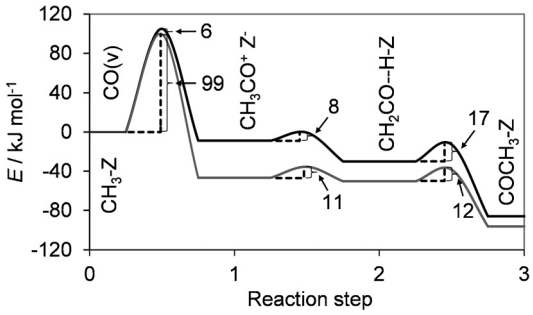

Figure 1. Reaction paths for formation of acetyl from a methyl group and CO within the 12-MR on T1-O4 and the 8-MR on T3-O3. Reaction steps: 0. CO in vacuum, methyl group on the zeolite; 1. acetyl carbocation and negatively charged zeolite; 2. ketene physisorbed onto a Brønsted acid site; 3. acetyl group on zeolite. Black line: reaction steps in the main channel (T1-O4); gray line: reaction steps in the side pocket (T3-O3).

and the optimized geometries of the reaction steps and transition states are shown in Figure 2. Among the sites in the 8-MR the energy barrier for this step is 7 kJ mol^{-1} lower at T3-O8 than at T3-O3, but the methyl group at T3-O8 is, in contrast, 11 kJ mol^{-1} less stable than that at T3-O3. A definite conclusion about the relative importance of these two sites would thus require a full micro-kinetic model. Next, the acetyl carbocation can react to form ketene which is physisorbed on a Brønsted acid site [Eq. (6)]. This reaction occurs with a low barrier (T1-O4: 8 kJ mol^{-1}, T3-O3: 11 kJ mol^{-1}). Alternatively, the acetyl carbocation can react directly to give the acetyl. This reaction involves a simple translational transition state with a very low-energy barrier (T1-O4: 2 kJ mol^{-1}, T3-O3: 1 kJ mol^{-1}, T3-O8: 20 kJ mol^{-1}). Both possibilities involve very low energy barriers, and the carbocation is therefore expected to be short-lived. It thus seems reasonable that the carbocation escaped detection in the NMR study by Corma and co-workers.[9] The ketene on the Brønsted acid site is restructured to acetyl [Eq. (7)]. This reaction also occurs with a low barrier (12-MR: 17 kJ mol^{-1}, 8-MR: 12 kJ mol^{-1}), and the steady-state concentration of ketene is thus also expected to be very low.

$$CH_3CO^+\text{-}[SiOAl]^- \rightarrow CH_2CO\text{-}[SiO(H)Al] \quad (6)$$

$$CH_2CO\text{-}[SiO(H)Al] \rightarrow [SiO(COCH_3)Al] \quad (7)$$

The results of our DFT calculations are summarized in Figure 1 and show that ketene is a potential reaction intermediate in both the 8-MR and the 12-MR. Additionally, we show that formation of acetyl is significantly faster in the 8-MR than in the 12-MR (the 6 kJ mol^{-1} difference in barrier translates into a factor of about 5 on the rates at 438 K) in good agreement with previous experimental and theoretical studies.[3,8b]

To evaluate the prediction of the DFT model wherein ketene is a reaction intermediate, we experimentally investigated whether ketene is present in the system. To detect the ketene experimentally, we introduced D_2O into the CO/DME feed after the MA synthesis had been given 5.7 hours to approach a steady state. The essential part of the experiment is that the gas-phase ketene is the only species in the system which will form doubly deuterated acetic acid upon introduction of deuterated water [Eq. (8)]:

$$C_2H_2O + D_2O \rightarrow CH_2DCOOD \quad (8)$$

It is well established that ketene reacts readily with D_2O in this way already at room temperature.[10] The other possible pathways to acetic acid formation, such as acetyl hydration, MA hydrolysis, and MeOH carbonylation [Eq. (9) to (12)] all result in acetic acid isotopes with, at most, a single deuterium atom.

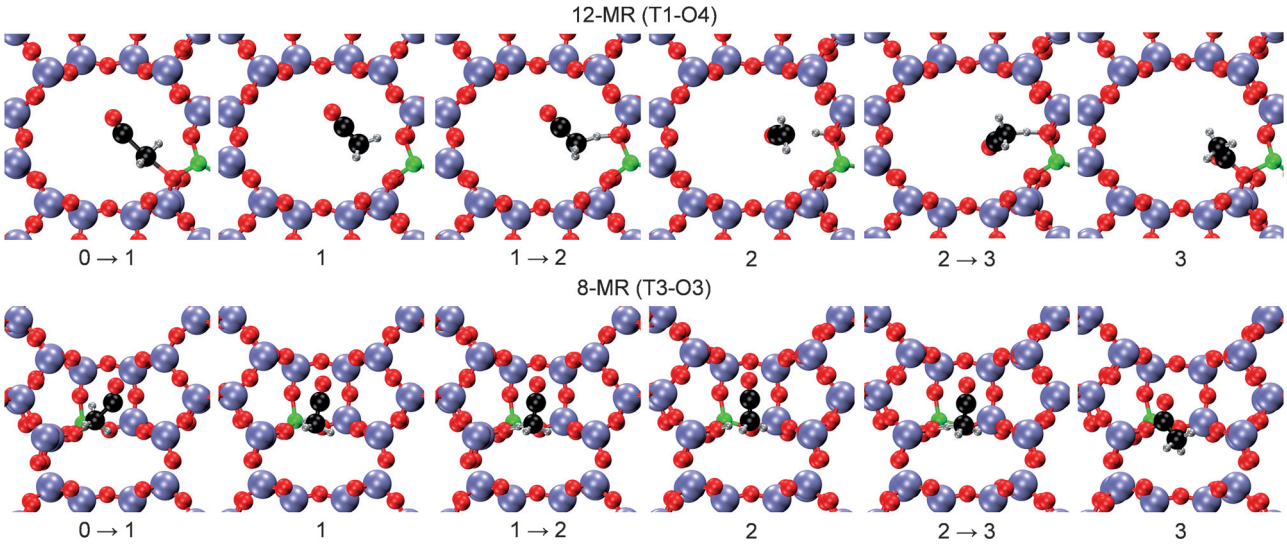

Figure 2. The optimized structures of the reaction intermediates and transition states for the reaction of CO with a methyl group in the 12-MR main channel (top) and in the 8-MR side pocket (bottom). Reaction steps: 0. CO in vacuum, methyl group on the zeolite; 1. acetyl carbocation and negatively charged zeolite; 2. ketene physisorbed onto a Brønsted acid site; 3. acetyl group on zeolite. Arrows indicate transition states. O red, Si blue, H gray, C black, Al green.

$$D_2O + [SiO(COCH_3)Al] \rightarrow CH_3COOD + [SiO(D)Al] \quad (9)$$

$$D_2O + CH_3OCH_3 \rightarrow 2\,CH_3OD \quad (10)$$

$$D_2O + CH_3COOCH_3 \rightarrow CH_3COOD + CH_3OD \quad (11)$$

$$CH_3OD + CO \rightarrow CH_3COOD \quad (12)$$

A distinction between the isomers is possible because previous isotopic studies have shown that the methyl groups are not deprotonated over acidic zeolites by either MeOH, DME, or D_2O, and scrambling of methyl protons does therefore not occur.[11b,11] Consequently, ketene is the only potential source of CH_2DCOOD (molar mass 62 u), while other routes to acetic acid lead to CH_3COOD (molar mass 61 u). We have therefore used mass spectrometry to test if CH_2DCOOD is produced when D_2O is introduced. To avoid that the crossover between adjacent masses in the mass detection leads to an erroneous conclusion, we do not base the analysis on absolute signals, but rather on the $m/z = 62$ to $m/z = 61$ mass ratio.

During the first 5.7 hours of the experiment (Figure 3) the rate of MA synthesis gradually increased, whereas the rate of methanol synthesis concurrently decreased. Then, D_2O was

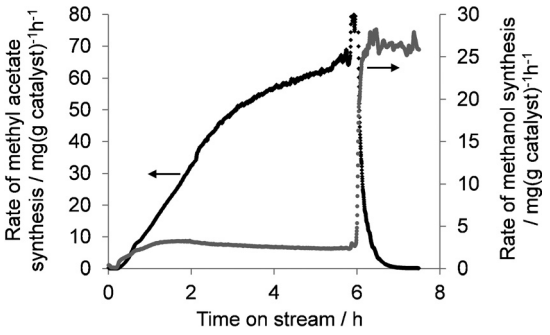

Figure 3. The rate of methyl acetate and methanol formation on H-MOR. Conditions: 9.8 bar CO, 0.2 bar DME, 300 Nml min^{-1}, 3.0 g catalyst, 438 K.

introduced into the CO/DME feed, at a constant flow of 0.01 mL min^{-1}, which corresponds to 4 mol % of the total reactant flow. Upon the introduction of deuterated water the carbonylation reaction was terminated by removal of the methyl groups as CH_3OD [Eq. (2) in the reverse direction], and the MA production stopped. Figure 4 shows the mass ratio between $m/z = 62$ (CH_2DCOOD) and $m/z = 61$ (CH_3COOD) as a function of time on stream during the experiment (the raw $m/z = 62$ and $m/z = 61$ signals are shown in Figure S4).

Before the addition of D_2O into the system, the ratio between the signals from doubly and singly deuterated acetic acid isotopes was a noise signal, but as D_2O was introduced, a well-defined peak emerged (the result of a control experiment with H_2O is shown in the SI). The peak in the mass ratio can be rationalized in terms of our theoretical model. Ketene is an intermediate in the carbonylation of DME to MA. Immediately upon the introduction of D_2O the carbonylation

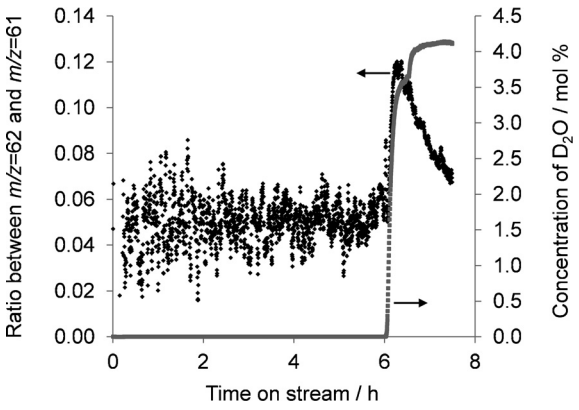

Figure 4. The ratio between the MS signal at $m/z = 62$ (doubly deuterated acetic acid) and $m/z = 61$ (singly deuterated acetic acid). Reaction conditions: 9.8 bar CO, 0.2 bar DME, 300 Nml min^{-1}, 3.0 g catalyst, 438 K.

reaction was still running, and ketene intermediates were available for conversion into CH_2DCOOD [Eq. (8)], whereby the $m/z = 62$ signal became more prominent. However, as shown in Figure 3, deuterated water also suppressed the carbonylation reaction by removing the essential methyl groups on the zeolite [Eq. (2) in the reverse direction], and when the carbonylation reaction thus stopped, and no more ketene intermediate was formed, the $m/z = 62$ signal from CH_2DCOOD dropped towards the noise level.

In conclusion, we have presented a theoretical DFT model of unprecedented detail for the carbonylation of DME over Mordenite zeolites. The theoretical model predicts the involvement of a ketene intermediate, which was not previously known to be involved in the reaction. We have experimentally identified ketene, which verifies our theoretical model. However, in addition to substantiating the DFT model, the observation of the highly reactive ketene molecule is also important because of its potential implications for zeolite catalysis. As an example, ketene undergoes base-catalyzed polymerization into polyketones at very low temperatures.[12] Ketene could therefore be of importance for the build-up of coke and larger carbonaceous structures which deactivate the catalyst in the carbonylation reaction. The observation of ketene is potentially also important for the ongoing fundamental studies of the formation of the initial C–C bonds using acidic zeolite catalysts for hydrocarbon synthesis.[13]

Experimental Section

All DFT calculations in this study were performed using the grid-based, projector augmented wave, DFT program GPAW and the ASE program package.[14] A grid spacing of less than 0.18 Å was used and the reciprocal space was sampled by a (1,1,2)-mesh of Monkhorst-Pack k-points. The exchange-correlation energy and potential were calculated within the generalized gradient approximation with the BEEF-vdW functional.[4] The transition states were found with the climbing-image NEB method and confirmed by frequency analysis using a displacement of 0.02 Å (see Table S2).[15] The structures and reaction paths were optimized until the residual force, acting on the atoms, was below 0.03 eV Å^{-1}.

Mordenite ($SiO_2/Al_2O_3 = 20$) was obtained from Zeolyst (CBV21A). The initial ammonium form was converted to the protonated form by heating it at 773 K for 3 h (heating rate 1 K min^{-1}) in a flow of dry air (300 Nml min^{-1}). Before the experiment, the catalyst (3.00 g, 125–250 μm) was calcined in the reactor at 773 K in a flow (300 Nml min^{-1}) of 10 % O_2 in N_2 for 3 h (heating rate 1 K min^{-1}) and cooled to the reaction temperature. The experiment was conducted in a high-pressure fixed-bed reactor,[16] in which the catalyst was loaded in a quartz tube (OD 10 mm, ID 8 mm). The carbonylation reaction was performed using 2 % DME in CO (AGA) at a flow of 300 Nml min^{-1}, 438 K and 10 bar. Deuterated water (Sigma–Aldrich, 99.9 atom % D), was added by an HPLC pump (Gilson, Model 305, 5SC pump head). The reactor effluent was transferred by heated lines to a mass spectrometer (Hiden Analytical QGA) and to a gas chromatograph (Agilent Technologies, model 6890N) equipped with a DB1 column connected to flame-ionization detector and a Porapak N column, followed by a 13x Molesieve column, connected to a thermal conductivity detector.

Keywords: carbonylation · density functional calculations · heterogeneous catalysis · reaction mechanisms · zeolites

How to cite: *Angew. Chem. Int. Ed.* **2015**, *54*, 7261–7264
Angew. Chem. **2015**, *127*, 7369–7372

[1] a) P. Cheung, A. Bhan, G. J. Sunley, E. Iglesia, *Angew. Chem. Int. Ed.* **2006**, *45*, 1617–1620; *Angew. Chem.* **2006**, *118*, 1647–1650; b) P. Cheung, A. Bhan, G. J. Sunley, D. J. Law, E. Iglesia, *J. Catal.* **2007**, *245*, 110–123; c) J. Liu, H. Xue, X. Huang, Y. Li, W. Shen, *Catal. Lett.* **2010**, *139*, 33–37.

[2] a) J. L. Liu, H. F. Xue, X. M. Huang, P. H. Wu, S. J. Huang, S. B. Liu, W. J. Shen, *Chin. J. Catal.* **2010**, *31*, 729–738; b) H. F. Xue, X. M. Huang, E. Ditzel, E. S. Zhan, M. Ma, W. J. Shen, *Ind. Eng. Chem. Res.* **2013**, *52*, 11510–11515; c) H. F. Xue, X. M. Huang, E. Ditzel, E. S. Zhan, M. Ma, W. J. Shen, *Chin. J. Catal.* **2013**, *34*, 1496–1503; d) H. F. Xue, X. M. Huang, E. S. Zhan, M. Ma, W. J. Shen, *Catal. Commun.* **2013**, *37*, 75–79.

[3] A. Bhan, A. D. Allian, G. J. Sunley, D. J. Law, E. Iglesia, *J. Am. Chem. Soc.* **2007**, *129*, 4919–4924.

[4] J. Wellendorff, K. T. Lundgaard, A. Møgelhøj, V. Petzold, D. D. Landis, J. K. Nørskov, T. Bligaard, K. W. Jacobsen, *Phys. Rev. B* **2012**, *85*, 235149.

[5] R. Y. Brogaard, P. G. Moses, J. K. Norskov, *Catal. Lett.* **2012**, *142*, 1057–1060.

[6] R. Y. Brogaard, R. Henry, Y. Schuurman, A. J. Medford, P. G. Moses, P. Beato, S. Svelle, J. K. Norskov, U. Olsbye, *J. Catal.* **2014**, *314*, 159–169.

[7] C. Baerlocher, L. B. McCusker, Database of Zeolite Structures: http://www.iza-structure.org/databases/.

[8] a) M. Boronat, C. Martinez-Sanchez, D. Law, A. Corma, *J. Am. Chem. Soc.* **2008**, *130*, 16316–16323; b) M. Boronat, C. Martinez, A. Corma, *Phys. Chem. Chem. Phys.* **2011**, *13*, 2603–2612.

[9] I. Lezcano-González, J. A. Vidal-Moya, M. Boronat, T. Blasco, A. Corma, *Angew. Chem. Int. Ed.* **2013**, *52*, 5138–5141; *Angew. Chem.* **2013**, *125*, 5242–5245.

[10] a) W. Caminati, F. Scappini, G. Corbelli, *J. Mol. Spectrosc.* **1979**, *75*, 327–332; b) T. F. Kahan, T. K. Ormond, G. B. Ellison, V. Vaida, *Chem. Phys. Lett.* **2013**, *565*, 1–4.

[11] a) D. M. Marcus, K. A. McLachlan, M. A. Wildman, J. O. Ehresmann, P. W. Kletnieks, J. F. Haw, *Angew. Chem. Int. Ed.* **2006**, *45*, 3133–3136; *Angew. Chem.* **2006**, *118*, 3205–3208; b) Z. M. Cui, Q. Liu, S. W. Baint, Z. Ma, W. G. Song, *J. Phys. Chem. C* **2008**, *112*, 2685–2688.

[12] a) G. Natta, G. Mazzanti, G. Pregaglia, M. Binaghi, M. Peraldo, *J. Am. Chem. Soc.* **1960**, *82*, 4742–4743; b) P. Zarras, O. Vogl, *Prog. Polym. Sci.* **1991**, *16*, 173–201; c) H. Egret, J. P. Couvercelle, J. Belleney, C. Bunel, *Eur. Polym. J.* **2002**, *38*, 1953–1961.

[13] a) J. E. Jackson, F. M. Bertsch, *J. Am. Chem. Soc.* **1990**, *112*, 9085–9092; b) J. F. Haw, W. G. Song, D. M. Marcus, J. B. Nicholas, *Acc. Chem. Res.* **2003**, *36*, 317–326; c) D. Lesthaeghe, V. Van Speybroeck, G. B. Marin, M. Waroquier, *Ind. Eng. Chem. Res.* **2007**, *46*, 8832–8838; d) U. Olsbye, S. Svelle, M. Bjorgen, P. Beato, T. V. W. Janssens, F. Joensen, S. Bordiga, K. P. Lillerud, *Angew. Chem. Int. Ed.* **2012**, *51*, 5810–5831; *Angew. Chem.* **2012**, *124*, 5910–5933.

[14] a) S. R. Bahn, K. W. Jacobsen, *Comput. Sci. Eng.* **2002**, *4*, 56; b) J. J. Mortensen, L. B. Hansen, K. W. Jacobsen, *Phys. Rev. B* **2005**, *71*, 035109; c) J. Enkovaara, C. Rostgaard, J. J. Mortensen, J. Chen, M. Dulak, L. Ferrighi, J. Gavnholt, C. Glinsvad, V. Haikola, H. A. Hansen, H. H. Kristoffersen, M. Kuisma, A. H. Larsen, L. Lehtovaara, M. Ljungberg, O. Lopez-Acevedo, P. G. Moses, J. Ojanen, T. Olsen, V. Petzold, N. A. Romero, J. Stausholm-Moller, M. Strange, G. A. Tritsaris, M. Vanin, M. Walter, B. Hammer, H. Hakkinen, G. K. H. Madsen, R. M. Nieminen, J. K. Norskov, M. Puska, T. T. Rantala, J. Schiotz, K. S. Thygesen, K. W. Jacobsen, *J. Phys. Condens. Matter* **2010**, *22*, 253202.

[15] G. Henkelman, B. P. Uberuaga, H. Jonsson, *J. Chem. Phys.* **2000**, *113*, 9901–9904.

[16] J. M. Christensen, P. M. Mortensen, R. Trane, P. A. Jensen, A. D. Jensen, *Appl. Catal. A* **2009**, *366*, 29–43.

Received: November 12, 2014
Revised: April 13, 2015
Published online: May 12, 2015

